PRAMANA
— journal of
physics

© Printed in India

Vol. 44, No. 2,
February 1995
pp. 85–108

A new computation scheme for triangular quantum billiards

PAOLO BELLOMO
School of Physics, Georgia Institute of Technology, Atlanta, Georgia, 30332-0430, USA

MS received 6 August 1994; revised 26 October 1994

Abstract. A new scheme for computing the eigenvalues and eigenstates of the Laplacian with Dirichlet boundary conditions on arbitrary triangular domains is presented. Its reliability is tested by comparing numerical results with analytical ones whenever possible. The computation of eigenvalues shows a good agreement with analytical results. The procedure is shown to give accurate results also in the case of eigenfunctions computation. Finally, the sensitivity of our scheme to the geometry of the domain is discussed and the algorithm is shown to detect small changes in the shape of the domain.

Keywords. Quantum billiards; spectral statistics; pseudointegrable systems, quantum chaos; eigenvalues computation.

PACS Nos 03·65; 05·45; 41·20

1. Introduction

In recent years the investigation of quantum eigenvalues–eigenstates of classically chaotic quantum systems has attracted much attention. Many (for an extensive set of references see [1]) have tried to identify quantum universalities that can be considered as fingerprints of classical chaos in the fully quantum regime. The numerical quantization of classically nonintegrable systems has been performed using diverse strategies and billiard quantization has become a common ground for computational studies in the field. In fact, classical billiards are capable of showing the whole panoply of dynamical properties: integrability, pseudointegrability, ergodicity (only) and chaos; and the restricted set of triangular billiards encompasses all the properties of the wider category of arbitrary convex polygonal billiards [2]. Billiard quantization has so far been carried out by many authors in many ways: Sinai billiard was quantized by Berry [3] by converting the problem into a band structure one; Bunimovich's stadium [4] was first solved by McDonald and McDonald and Kaufman [5], using the Green function method developed by Riddel [6, 7], and later tackled by Heller [8] who used a superposition of systematically oriented plane waves to represent the eigenfunctions of the laplacian. Cheon and Cohen [9] studied a pseudointegrable approximation to Sinai billiard by replacing the infinite walls of their billiard with a very large, but finite, potential barrier; Biswas and Jain [10] also employed Riddel's algorithm in the quantization of the $(\pi/3)$-rhombus billiard.

The present work describes the quantization of arbitrary triangular quantum billiards. The solution of such a problem is particularly interesting because of the paradigmatic nature of triangular billiards (they can exhibit all the properties including the "A-integrability" concept [11]). Moreover the analytical solutions for the few exactly integrable cases are known (equilateral triangle, half equilateral triangle, half

square) and they provide a confidence test for numerical results. Surprisingly enough, in spite of the suitability of triangular billiards for the study of many interesting phenomena such as eigenvalue statistics [1], investigation of scars [8, 12] and the relationship between periodic orbits and quantization [13], to the best of our knowledge no systematic calculation of both their eigenvalues and eigenfunctions exists; the majority of numerical studies of quantum billiard spectra was so far dedicated to the investigation of classically chaotic examples (triangular billiards can be at most only ergodic). Finally, we want to point out that recent experiments in microwave resonators have put triangular quantum billiards within the realm of experimental nonlinear dynamics [14].

It is therefore our intent to give a very detailed account of our solution in the hope of stimulating systematic investigations both of the properties of the spectra of arbitrary triangular quantum billiards and, more specifically, of the characteristics of their eigenfunctions. A first application of the scheme is given in [12, 15]. The same scheme can be also used to solve the problem of a triangular billiard with some non-singular potential. Our numerical scheme is very easy to apply: it is simple and effective; it requires surprisingly small computation times and, as we show in the following paragraphs, it provides very accurate results for the billiard eigenfunctions.

2. Representation of the quantum billiard operator

By a rescaling of the physical constants, the quantum billiard problem can be reduced to the following equation and boundary conditions

$$\begin{aligned} &-\nabla^2\psi(x,y)=\lambda\psi(x,y),\\ &\mathbf{q}\in\partial\mathcal{Q}\Rightarrow\psi(\mathbf{q})=0,\\ &\psi(\mathbf{q})\in\mathcal{L}^2(\mathcal{Q}), \end{aligned} \tag{1}$$

where $\partial\mathcal{Q}$ denotes the boundary of the domain considered. In this paper we refer to the "*quantum billiard operator*" (henceforth denoted QBO) as a shorthand for the operator of Eq. (1). We stress here that the QBO is not merely the laplacian, because the vanishing of the functions on the boundary of the billiard is required (*Dirichlet* boundary conditions). We will indicate the QBO as $-\nabla^2_{\partial\mathcal{Q}}$.

The solution presented in this paper makes use of a matrix representation, properly truncated, of the QBO. By a judicious choice of the Hilbert space vectors employed in the construction of the matrix, we were able to take into account the proper boundary conditions (i.e. vanishing of the wave functions on the sides of the triangle) and therefore to construct a *faithful* representation of the QBO. The desired matrix elements are of the form

$$\mathcal{D}_{i,j}=\langle i|-\nabla^2_{\partial\mathcal{Q}}|j\rangle, \tag{2}$$

where $|i\rangle$, $|j\rangle$ must be vectors belonging to some complete set of orthonormal functions, $\mathcal{L}^2$-integrable on the domain $\mathcal{Q}$ and satisfying the boundary conditions (1). The Hamiltonian operator is linear and real, and the eigenfunctions can always be made real-valued; therefore in what follows we will neglect complex conjugation. The construction of the desired basis vectors is best illustrated in a two-step procedure. We begin by considering the eigenfunctions of the QBO on a unit square [16]

$$\psi^{\text{square}}_{m,n}(x,y)=2\sin(m\pi x)\sin(n\pi y), \tag{3}$$

with m and n being some arbitrary nonzero integers. By antisymmetrization with respect to a diagonal, one can form the eigenfunctions of the QBO on the half unit square domain, i.e. on a $((\pi/4), (\pi/4), (\pi/2))$-triangle, having its $(\pi/2)$ angle vertex sitting in the origin of the frame of reference [16]

$$\psi_{m,n}^{((\pi/4),(\pi/4),(\pi/2))}(x, y) = 2\{\sin(m\pi x)\sin(n\pi y) + (-1)^{m+n+1}\sin(n\pi x)\sin(m\pi y)\}. \tag{4}$$

Indices n and m must obey an additional constraint: $n \neq m$. We now consider the eigenfunctions of the QBO on a rectangle of side lengths a and b respectively [they are a generalization of (3)]

$$\psi_{m,n}^{\text{rectangle}}(x, y) = \frac{2}{\sqrt{ab}}\sin\left(\frac{m\pi x}{a}\right)\sin\left(\frac{n\pi y}{b}\right). \tag{5}$$

Next we apply the same antisymmetrization and we obtain the following set of functions

$$\phi_{m,n}(x, y) = \frac{2}{\sqrt{ab}}\left\{\sin\left(\frac{m\pi x}{a}\right)\sin\left(\frac{n\pi y}{b}\right) + (-1)^{m+n+1}\sin\left(\frac{n\pi x}{a}\right)\sin\left(\frac{m\pi y}{b}\right)\right\}. \tag{6}$$

Once again, $n \neq m$ is required. Clearly, the $\phi_{m,n}(x, y)$'s are not eigenfunctions of the QBO on the half rectangle, because $a \neq b$; nevertheless they constitute a complete set of orthonormal functions, as we are going to prove. Let us denote by $\mathcal{Q}_1$ the triangle defined by the diagonal of the rectangle and having its $(\pi/2)$ angle placed in the origin; by $\mathcal{Q}_2$ we denote the half unit square obtained from the former triangle upon a rescaling of the sides lengths $(x' = (x/a), y' = (y/b))$. We then consider the changes under such rescaling in the inner product of two functions (6)

$$\begin{aligned}\iint_{\mathcal{Q}_1} \phi_{m,n}(x, y)\phi_{i,j}(x, y)\mathrm{d}x\mathrm{d}y \\ = \frac{1}{ab}\iint_{\mathcal{Q}_2} \psi_{m,n}^{((\pi/4),(\pi/4),(\pi/2))}(x', y')\psi_{i,j}^{((\pi/4),(\pi/4),(\pi/2))}(x', y')\frac{\partial(x, y)}{\partial(x', y')}\mathrm{d}x'\mathrm{d}y'.\end{aligned} \tag{7}$$

Since the Jacobian of the transformation is $J = (\partial(x, y)/\partial(x', y')) = ab$, it is easy to see that we are left with the inner product of two normalized eigenfunctions of the QBO on the half unit square. They are eigenfunctions of a hermitian operator and therefore they are orthonormal to each other; this proves that functions (6) are orthonormal to each other also. In order to prove the completeness of the set, we consider some arbitrary, $\mathscr{L}^2$-integrable function $f(x, y)$ that vanishes on $\partial\mathcal{Q}_1$. By the same coordinate transformation we obtain

$$\begin{aligned}\iint_{\mathcal{Q}_1} \phi_{m,n}(x, y)f(x, y)\mathrm{d}x\mathrm{d}y \\ = \sqrt{ab}\iint_{\mathcal{Q}_2} \psi_{m,n}^{((\pi/4),(\pi/4),(\pi/2))}(x', y')f(ax', by')\mathrm{d}x'\mathrm{d}y'.\end{aligned} \tag{8}$$

If the left hand side of (8) vanishes for every pair (m, n), so does the right hand side; but the vanishing of the right hand side integral allows us to conclude that $f \equiv 0$, because the ψ's are a complete set for those functions like $f(ax, by)$ that vanish on $\partial\mathcal{Q}_2$. We conclude that the only function orthogonal to all the ϕ's is the null function, and this proves that the set is complete. In the next step we construct the basis set for the more general case of an arbitrary triangle.

Consider the following active transformation of the plane into itself

$$\begin{aligned} x' &= x + y\cdot\tan\gamma \\ y' &= y \end{aligned} \tag{9}$$

where $\gamma = (\pi/2) - \eta$ and η is the angle of the desired triangle with the vertex in the origin of the coordinate axes. Transformation (9) maps a rectangle into a parallelogram and therefore the half rectangle into an arbitrary triangle [see figure 1]. We now consider the functions

$$\chi_{m,n}(x, y) = \frac{2}{\sqrt{ab}}\left\{\sin\left[\frac{m\pi(x - y\cdot\tan\gamma)}{a}\right]\sin\left(\frac{n\pi y}{b}\right) + (-1)^{m+n+1}\sin\left[\frac{n\pi(x - y\cdot\tan\gamma)}{a}\right]\sin\left(\frac{m\pi y}{b}\right)\right\}; \tag{10}$$

which is the desired basis set. In fact, we only need to perform the inverse transformation of (9); any arbitrary triangle is mapped into some half rectangle which, in turn, can be mapped into a half unit square by rescaling the sidelengths. Clearly, the two transformations in sequence map the functions (10) into the eigenfunctions of the QBO on the half unit square. Orthonormality and completeness can then be proven by reducing every integral to an integration over the half unit square that involves eigenfunctions of the QBO on that domain (we still have $J = ab$). Moreover,

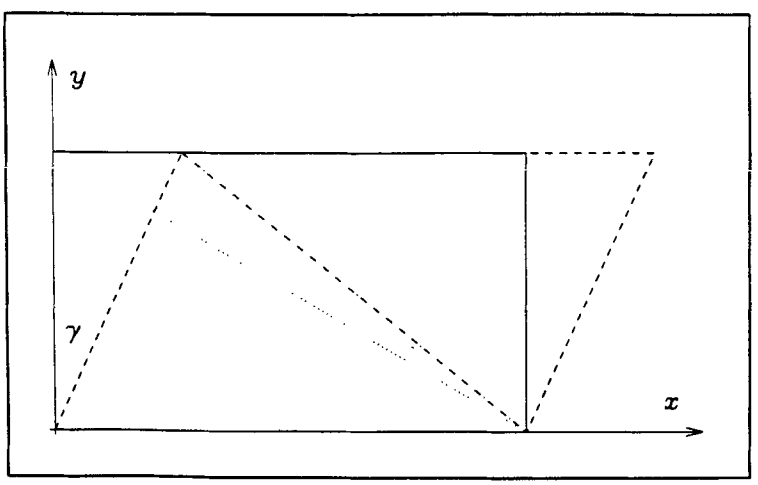

Figure 1. Under the affine transformation (9) a rectangle (solid line) is mapped into a parallelogram (dashed line); consequently its half is mapped into some triangle determined by the angle γ.

the mapping of the half unit square into an arbitrary triangle is linear and this guarantees that functions (10), being the image of eigenfunctions that vanish on the boundary of the half unit square, satisfy the Dirichlet boundary conditions.

We can now proceed to the construction of the matrix representation of the QBO (a detailed calculation of the matrix elements is reported in the appendix). In doing so some care must be taken about the ordering of the basis vectors, because functions (10) are labeled by a pair of indices rather than a single one. The most reasonable choice is to order the vectors according to the expectation value of the QBO

$$\langle -\nabla^2_{\partial\mathcal{L}} \rangle = \int\int_{\mathcal{L}} \chi_{m,n}(x,y)(-\nabla^2_{\partial\mathcal{L}})\chi_{m,n}(x,y)\mathrm{d}x\mathrm{d}y. \tag{11}$$

The expectation value above represents the energy content of a given vector, namely how rapidly the corresponding wave function oscillates. It is therefore sensible to expect that low energy eigenstates, i.e. relatively slowly varying eigenfunctions, do not have large projections on high energy vectors, i.e. rapidly oscillating functions. From the considerations above we assume that some proper truncation of the matrix can still yield satisfactory results, at least for the first few lowest lying eigenstates. Of course, the sole justification for such an assumption is the good agreement between numerical and analytical results in those cases in which the latter are available. The outcome of such a comparison is described in the next section, where we consider the analytical solution of (1) in an equilateral triangle.

3. Reliability of the solution

In this last section we present the comparison between numerical and analytical results. Not surprisingly, an analytical solution is available solely for those quantum billiards which are classically integrable. In the class of triangular billiards this amounts to the equilateral triangle, the half equilateral triangle and the half square. We applied our scheme to the equilateral triangle and compared our results with the analytical ones.

The quantum billiard in an equilateral triangle was first solved by Lamé [17], who was interested in the vibrating membrane problem; a mathematically rigorous solution of the same problem was recently published by Pinsky [18]. The eigenvalues of the QBO on the equilateral triangle with side length l are given by

$$E_{m,n} = \frac{16\pi^2}{27l^2}(m^2 + n^2 - mn), \tag{12}$$

where n and m are integers satisfying the following conditions

$$\begin{aligned} &n + m = 3k \quad k = \text{integer} \\ &m \neq 2n \\ &n \neq 2m. \end{aligned} \tag{13}$$

The case in which both $m = 0$ and $n = 0$ must also be ruled out. The (unnormalized) eigenfunctions are given by

$$\psi^{((\pi/3),(\pi/3),(\pi/3))}_{m,n}(x,y) = \sum_{(m,n)} \pm \exp\left[\left(\frac{2\pi i}{3l}\right)\left(nx + \frac{(2m-n)y}{\sqrt{3}}\right)\right]. \tag{14}$$

Exactly six (m, n) pairs must be considered in (14) and the rule is

$$(m, n) \to (m, m-n) \to (-n, m-n) \to (-n, -m) \to (n-m, -m) \to (n-m, n); \tag{15}$$

each transition induces a change of sign. We considered a triangle of side length $l = \pi$. The first test concerns eigenvalues computation: results are summarized in figure 2, where we compare the first 925 numerical eigenvalues (this corresponds to a maximal magnitude of the De Broglie wave vector $|\kappa| \sim 54$) with their analytical counterparts. In figure 2a we plot the logarithm in base 10 of the relative error versus $|\kappa|$, while in figure 2b we report the mean value of the same, again versus $|\kappa|$. Figure 2 shows good agreement with the analytical results, especially if one considers the small dimensions (2000 x 2000) of the matrix representing the QBO. Approximately half of the eigenvalues are an accurate approximation to the exact spectrum. In spite of the small dimensions of the matrix our results are very good up to a wavelength of the order of $\sim \frac{1}{25}$ of the side length. The eigenvalues considered in figure 2 were counted by taking degeneracy into account; this was done because when the method is applied to some asymmetric triangle there will be no degeneracy, and our counting

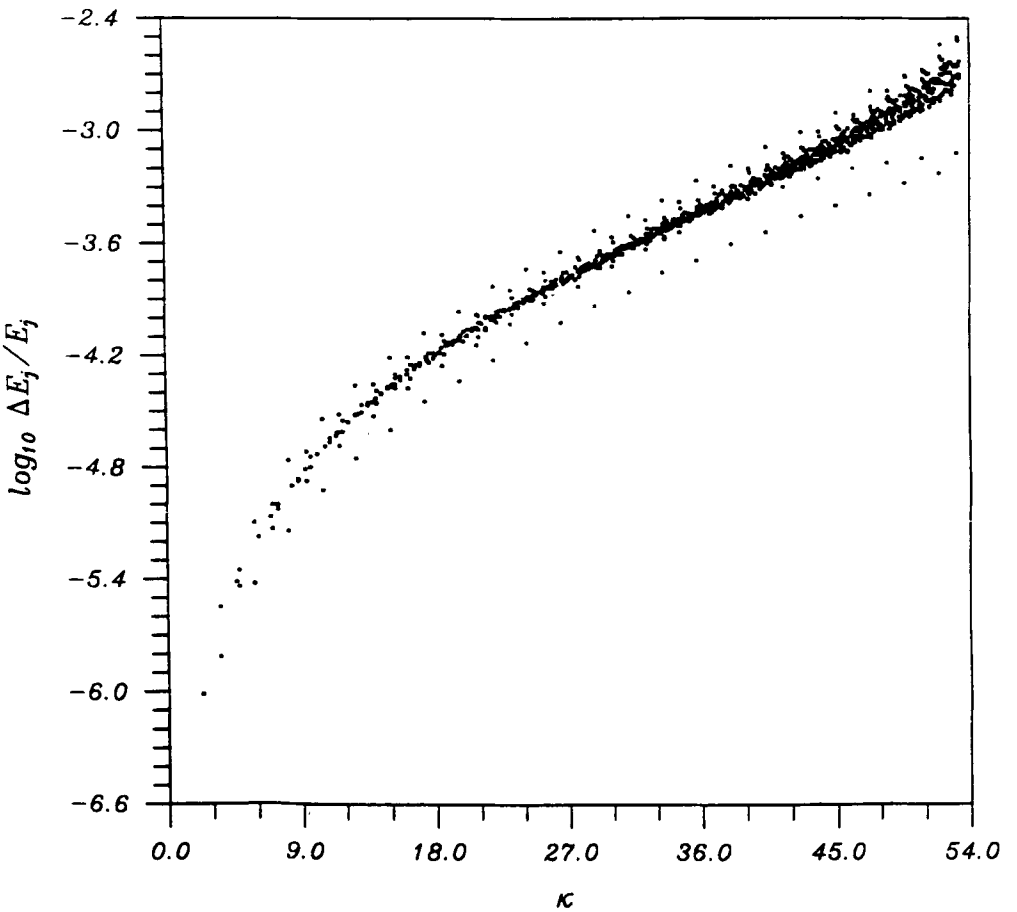

Figure 2(a).

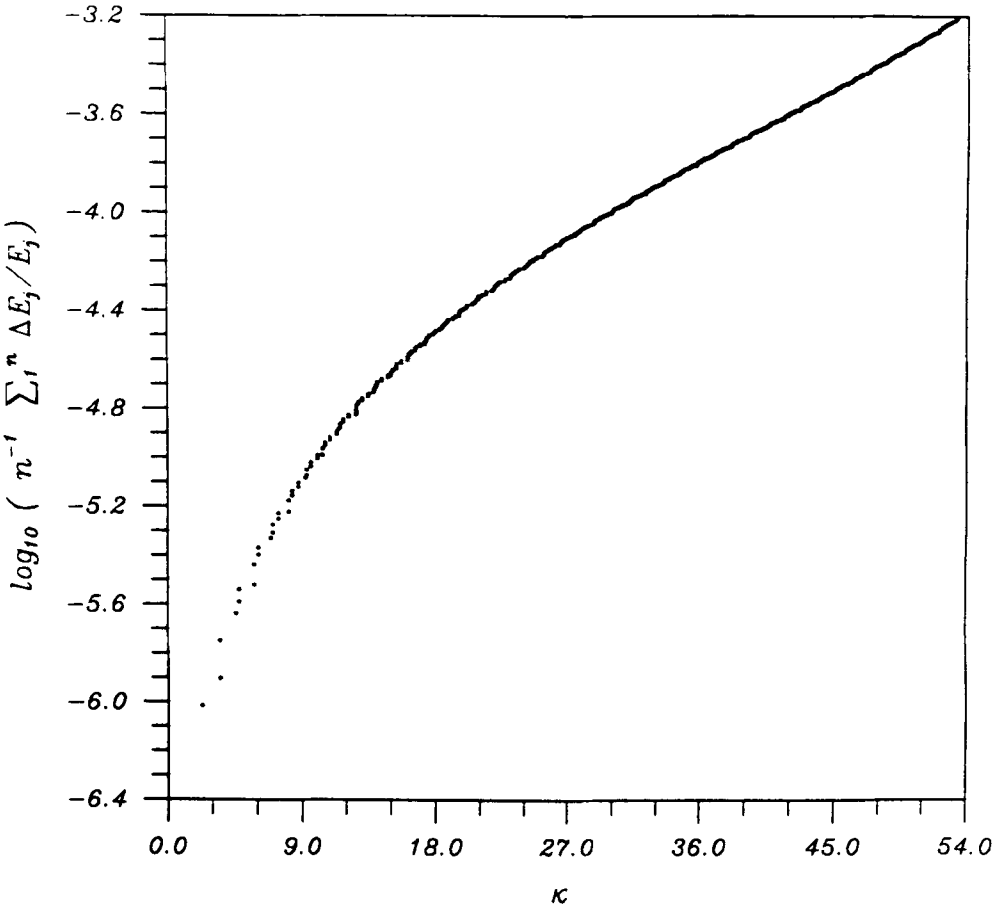

Figure 2(b).

Figure 2. Comparison between the numerical result and the analytical values for the spectrum of the equilateral triangle; (**a**) Logarithm (in base 10) of the relative error between the numerical eigenvalues and the exact ones vs. the magnitude of the wave vector **κ**; (**b**) Logarithm (in base 10) of the average error between numerical eigenvalues and analytical ones vs. the magnitude of the wave vector **κ**.

gives information about how many distinct eigenvalues can be computed, and their precision, in the case of some classically nonintegrable billiard. However, a moment's thought shows that such an estimate can hold only for triangles not too different from the equilateral one. Consider, for example, the half equilateral triangle: there, the same calculation, i.e. a matrix of the same dimensions, yields approximately half as many accurate eigenvalues, namely the energy levels of those equilateral triangle eigenstates which are odd under reflection about the height of the triangle. This is a consequence of Weyl's law for the integrated density of states $\mathcal{N}(E)$ which, including low energy corrections, reads [1]

$$\mathcal{N}(E) = \frac{A}{4\pi} E - \frac{L}{4\pi}\sqrt{E} + \Sigma c(\alpha_i) \tag{16}$$

with:

$$c(\alpha_i) = \frac{1}{2\pi}\left(\frac{\pi}{\alpha_i} - \frac{\alpha_i}{\pi}\right), \tag{17}$$

where L is the perimeter of the triangle and α_i is the ith internal angle. Weyl's law can be used as test for the results of any numerical calculation of billiard spectra. The equilateral triangle is a special billiard, therefore we performed Weyl's law test and verified the consistency of our scheme, also when applied to classically nonintegrable triangles. The results of the test are displayed in figures 3–4. Figure 3 refers to an irrational triangular billiard, with angles not very different from $(\pi/3)$: as expected the numerical staircase (solid line) fits well Weyl's law prediction (dashed line) up to $\sim$ the 950th eigenvalue, namely the same range of precision as for the equilateral triangle. Figure 4a, instead, refers to a pseudointegrable billiard, a $((\pi/10), (3\pi/10), (6\pi/10))$ triangle: in it one sees that the loss of precision occurs much earlier in terms of

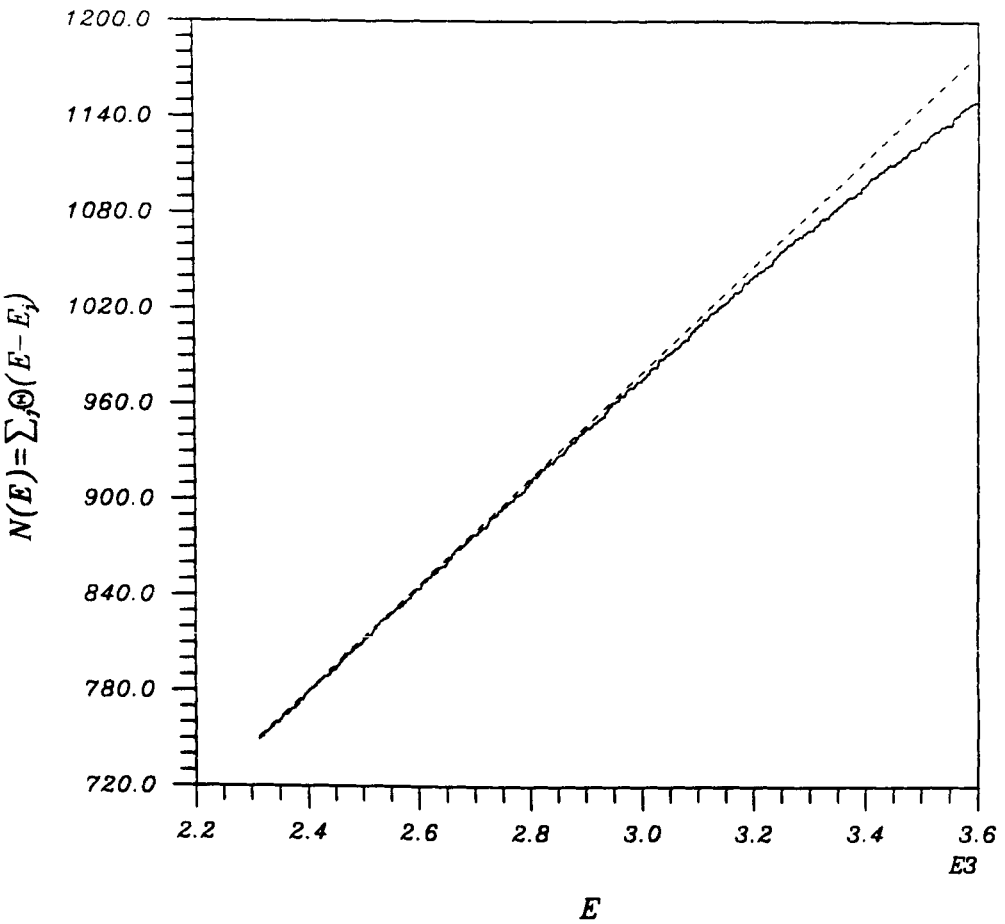

Figure 3. Analytical integrated density of states (dashed line) and numerical staircase (solid line) for an irrational billiard. The divergence between the two reflects the drop in the computational precision. For lower energies the two overlap and become indistinguishable on a coarse scale.

number of eigenvalues, but approximately in the same energy range as before. The range in which the calculation begins to lose precision is the one predicted by keeping the energy fixed and rescaling $\mathcal{N}(E)$ by the area of the billiard as required by Weyl's law; and the smaller number of accurate eigenvalues obtained in the pseudointegrable case is yet another example of the well-known difficulty in computing the spectra of narrow triangles [19]. For smaller energies than those presented in figures 3–4 the theoretical prediction and the numerical staircase overlap exactly. It is also interesting to observe that the onset of the divergence between the computed eigenvalues and the predictions of Weyl's law is very sharp, as it can be appreciated from figure 4b, where the relative deviation from the area rule for the same pseudointegrable triangle is plotted.

It is known that the Green function method allows a slightly better precision in the computation of the eigenvalues for a given matrix dimension, since one can concentrate all the computational power in the evaluation of a single eigenvalue. However, the method requires a scanning of the real axis which implies long computing times and the risk of missing some eigenvalues, and it cannot resolve degenerate eigenvalues. This is not the case for our scheme, which moreover requires surprisingly modest computing times (the matrix elements can be evaluated analytically; this

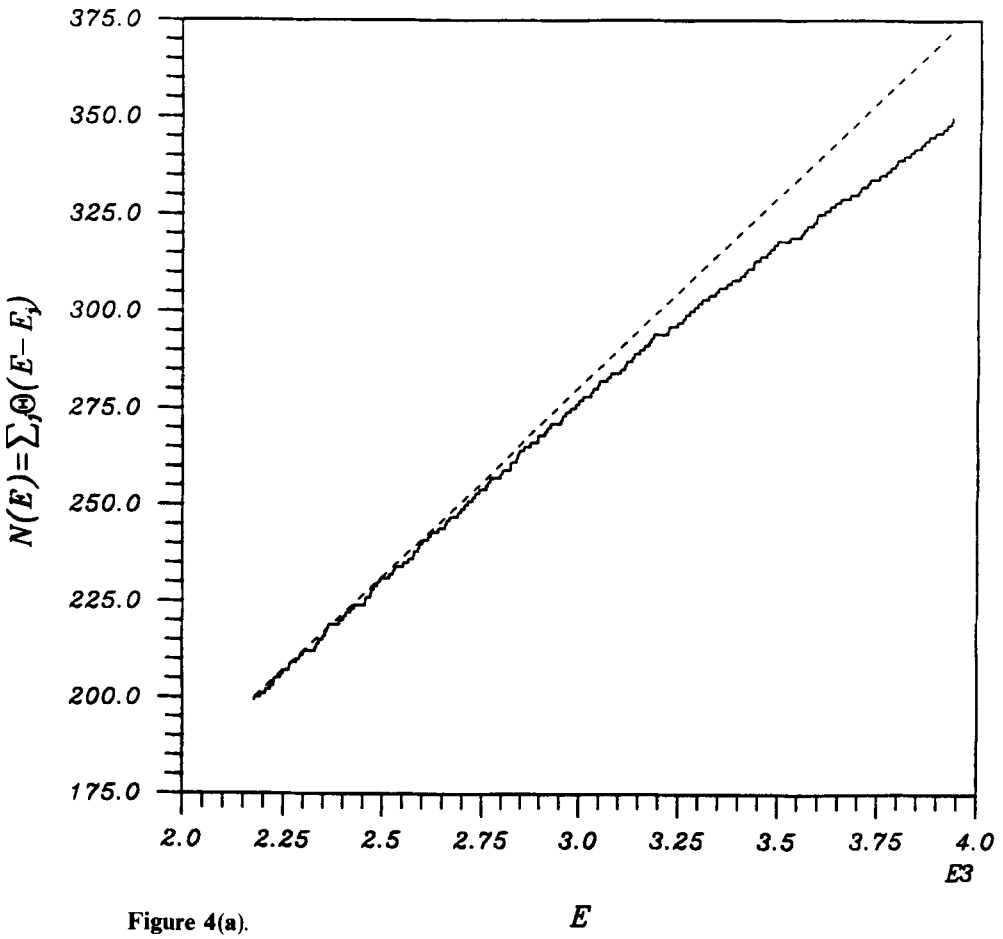

Figure 4(a).

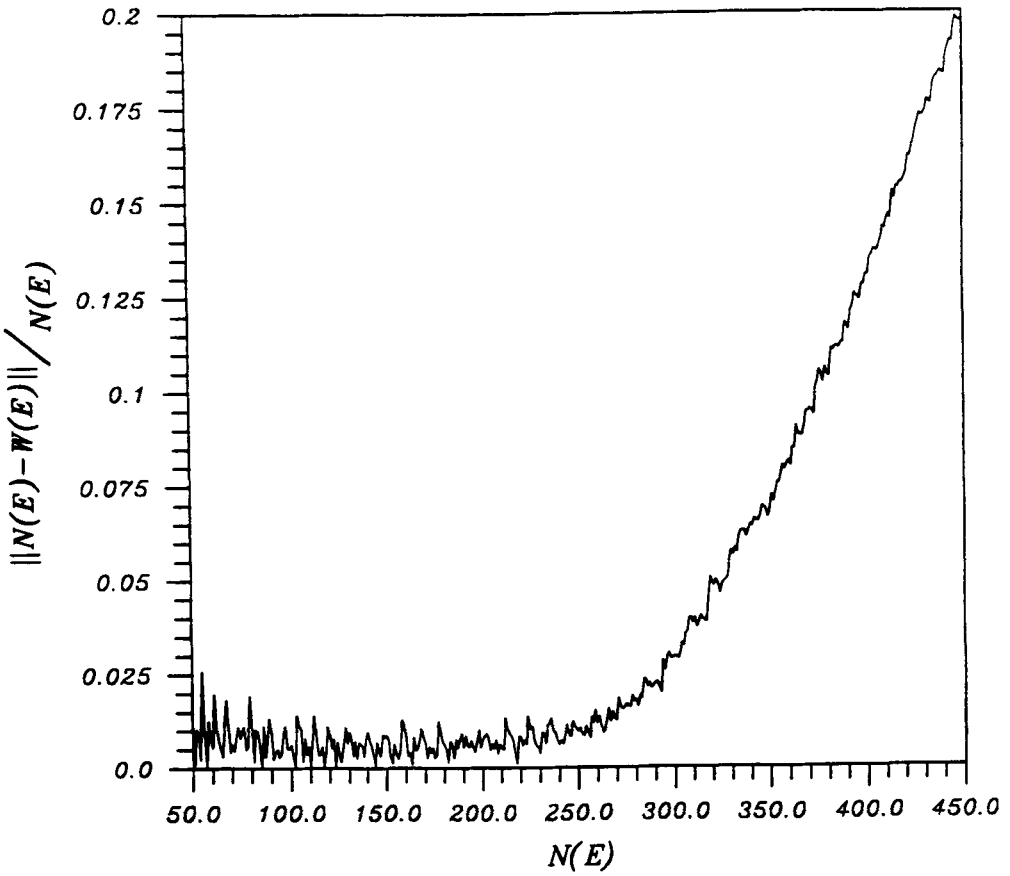

Figure 4(b).

Figure 4. Integrated density of states for a pseudointegrable ((π/10), (3π/10), (6π/10)) triangle; (**a**) Analytical integrated density of states (dashed line) and numerical staircase (solid line). The divergence between the two occurs after fewer states than in figure 3, but approximately in the same energy range; (**b**) Absolute value of the relative difference between the numerical staircase and the predictions of Weyl's law (plus corrections): the sudden onset of an exponential divergence is apparent.

shortens the time needed for the computation of the matrix dramatically). However, the main feature of our solution is the very good precision in the computation of the eigenfunctions. This is illustrated next.

In figure 5 we plot the value of the correlation integrals between numerical and analytical eigenfunctions up to the 380th eigenstate

$$I(j) = \int\int_{\mathcal{L}} \psi_j^{\text{analytical}}(x, y)\psi_j^{\text{numerical}}(x, y)\mathrm{d}x\mathrm{d}y. \tag{18}$$

From the form of Pinsky's [18] solution one can immediately deduce the existence of a double degeneracy due to the sine-cosine decomposition of the exponentials:

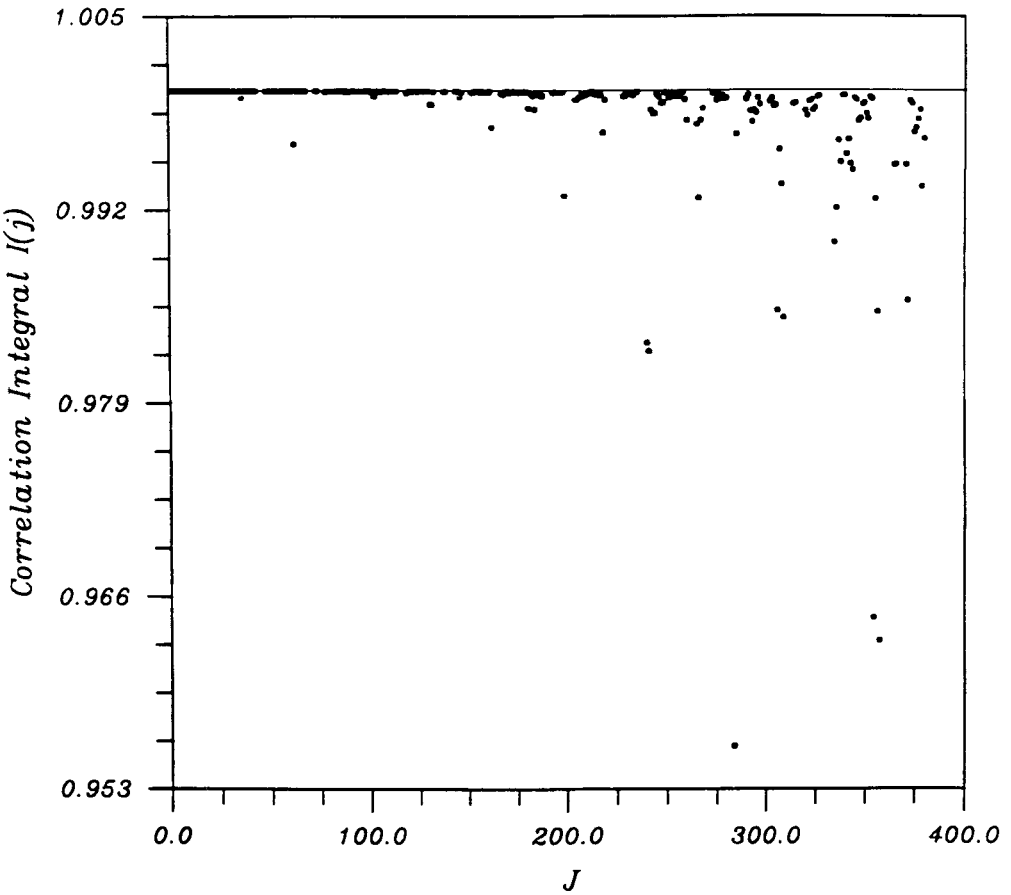

Figure 5. Correlation integrals between the first 380 normalized numerical eigenfunctions and their exact counterparts. The great accuracy of the computation is evident.

clearly, in (18) by $\psi_j^{\text{analytical}}$ we mean either sine or cosine (in the case $n = m$ there is no double degeneracy: the cosine solution vanishes identically). Figure 5 shows the high precision of our calculation. A more detailed account of it can be found in table 1, where the explicit values of $I(j)$ for the first 20 eigenfunctions are exhibited. Results of figure 5 and table 1 were evaluated semi-analytically: a numerically computed eigenfunction consists of a finite linear combination of the basis functions (10)

$$\psi_j^{\text{numerical}}(x, y) = \sum_{m,n} a_{m,n} \chi_{m,n}(x, y); \tag{19}$$

therefore integral (18) can be reduced to a summation of simpler terms

$$I(j) = \sum_{m,n} a_{m,n} \iint_{\mathcal{Q}} \psi_j^{\text{analytical}}(x, y) \chi_{m,n}(x, y) \mathrm{d}x \mathrm{d}y. \tag{20}$$

Each integral in (20) can be evaluated analytically, making the computation of $I(j)$

Table 1. Results of the correlation integral between the first 20 numerical and analytical wavefunctions of the equilateral triangle.

Table 1.	Correlation integrals.
1	0·9999998808
2	0·9999998235
3	0·9999997616
4	0·9999998808
5	0·9999996424
6	0·9999996424
7	0·9999993443
8	0·9999997616
9	0·9999994040
10	0·9999988079
11	0·9999998212
12	0·9999996424
13	0·9999989867
14	0·9999988675
15	0·9999991655
16	0·9999990463
17	0·9999992251
18	0·9999993443
19	0·9999958873
20	0·9999994636

precise and the test reliable. The results of figure 5 are particularly interesting because they were obtained diagonalizing a very small (1000 × 1000) matrix, which required very short computing times. In figure 5 the correlation integral is not plotted for every possible eigenfunction, the reason being that in some cases, besides the already mentioned sine-cosine degeneracy, there happens to be some higher degeneracy, due to the possibility of producing the same eigenvalue with two [or more] distinct pairs of integers. In the case of doubly degenerate solutions the algorithm yields naturally the same basis for the eigenspace as Pinsky's [18], which makes the correlation integral meaningful. On the other hand, for more highly degenerate eigenvalues the numerical calculation selects a different eigenspace basis. For example, for fourfold degenerate eigenvalues, the sine-cosine distinction is still preserved, but some mixing occurs between the two sine [or cosine] solutions related to the two distinct pairs of integers. Clearly, in such a situation a superposition integral does not give any useful information about the precision of the numerical results; however, by inspecting contour plots of proper linear combination of Pinsky's [18] eigenfunction, it was possible to recognise the consistency of our numerical results.

For eigenfunction computation there is no test (like a comparison with Weyl's law predictions) to verify the consistency of the results in the case of nonintegrable billiards. However, in figure 6a we plot the components along the basis vectors for the normalized 250th state of the same irrational billiard considered before. They were obtained by diagonalizing a 1000 × 1000 matrix. It is apparent that such components become very small as higher energy basis vectors are considered. This ensures (at a

reasonable degree of confidence: some large components along extremely energetic basis vectors might always exist) that our numerical calculation yields a very good approximation to the actual wave function. In figure 6b we plot the components for the 430th normalized eigenstate of the same billiard, which belongs to that range of the spectrum where the precision of the computation begins to drop (for the given dimension of the matrix). The interesting feature is the smallness of the first ~ 100 components, which implies that a representation of the QBO obtained by leaving out, say, the first 100 basis vectors and including 100 high energy functions (those ranging from the 1001st to the 1100th) would yield a better result. This observation suggests the possibility of scanning a large portion of the spectrum using a series of matrices centered on states of increasing energy. Such matrices would not be of fixed dimension (the increasing complexity of rapidly oscillating high energy eigenfunction would require a larger basis set) but they would still be relatively small. Note that, in a given application, not all the elements of expansion (19) need to be considered. In fact, once a threshold for the desired precision is fixed, all those coefficient in (19) that lead to contributions below that threshold can be dropped leading to some little computing time consuming expressoin for the eigenfunctions [which we actually did in many of our calculations].

Finally, we address the issue of the sensitivity of the scheme to change of the geometrical shape of the QBO domain. To this end, we first show in figure 7a one

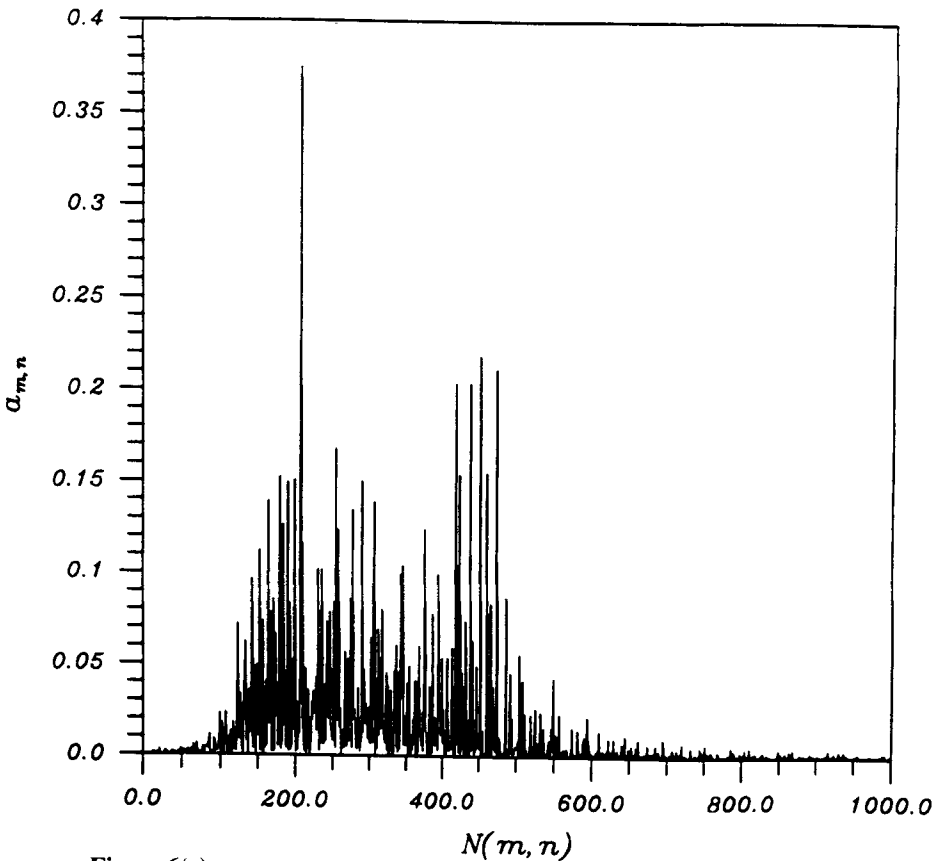

Figure 6(a).

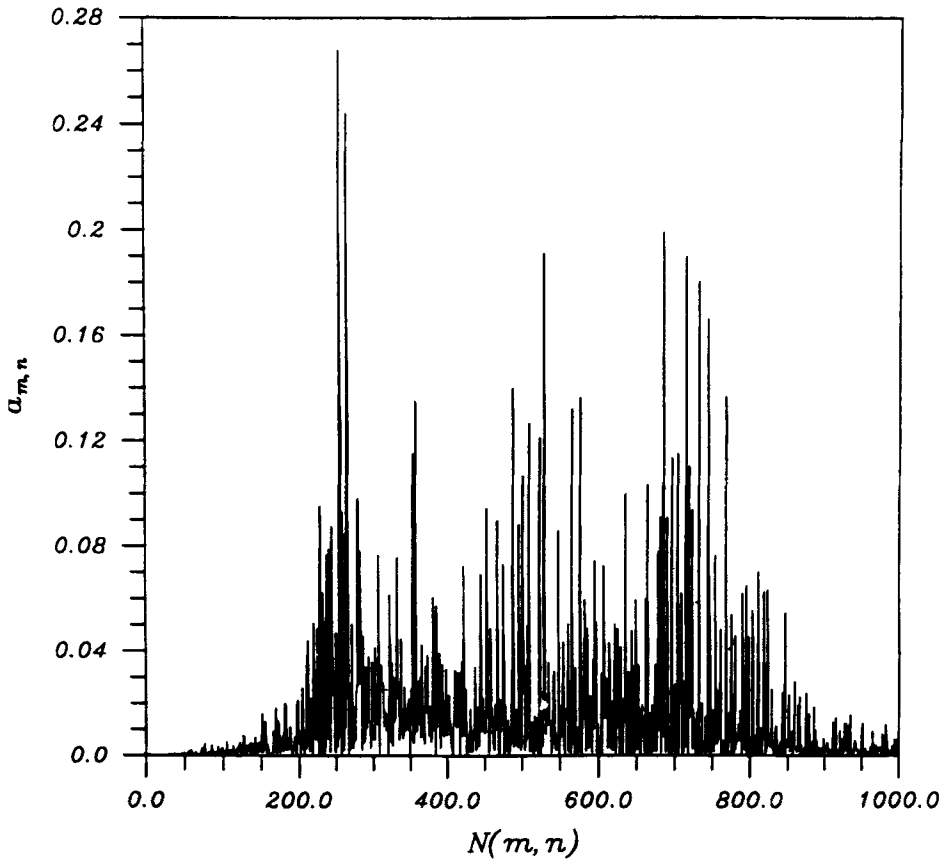

Figure 6(b).

Figure 6. Components of the eigenfunctions along the basis states; (**a**) 250th eigenstate: components become very small with increasing energy making the result very reliable; (**b**) 430th eigenstate: the projection on the lowest energy basis states is almost negligible, therefore a smaller matrix would still yield accurate results.

of the two first excited states (recall the double degeneracy) of the equilateral triangle, which was computed diagonalizing a 400×400 matrix. As expected a nodal line coincides with one of the bisectors of the triangle, specifically the one bisecting the angle the vertex of which sits at the origin of the frame of reference; in fact, we performed the computation placing the origin of the coordinates on the vertex which is labeled "α" in the figure. The relationship between the location of the nodal line and the position of the frame of reference is also shown in figure 7b, which refers to a calculation (again a 400×400 matrix) performed putting the origin of the coordinates on vertex "β". Next, we turned to the study of an isosceles triangle obtained by slightly stretching the height relative to the x-axis side of the equilateral triangle of figures 7a, 7b (a billiard which, to the best of our knowledge, nobody has ever investigated). For that eigenstate of the isosceles triangle that originates from the one of figures 7a and 7b, one expects from symmetry arguments that the nodal line lie along the longest height, independently of the location of the reference frame. We performed a calculation using a 400×400 matrix and placing the frame of

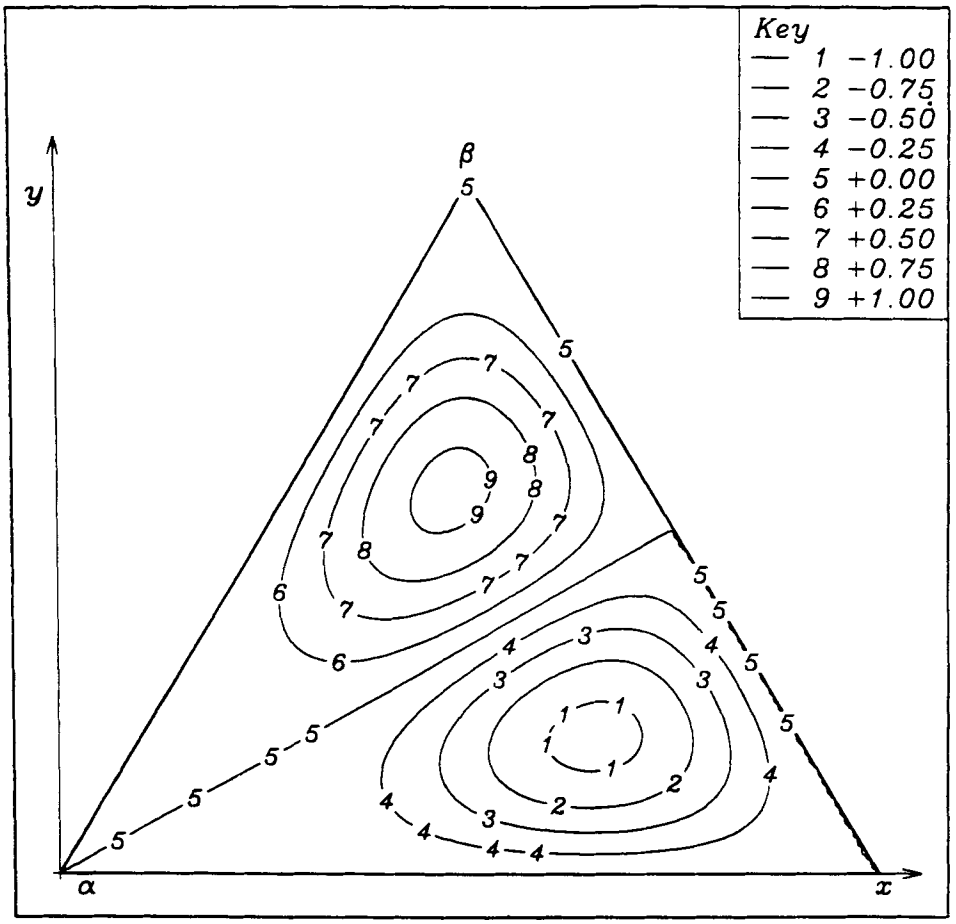

Figure 7(a).

reference on vertex "α", and we studied an isosceles triangle very close to the equilateral triangle, namely we stretched the height relative to the x-axis base only by 0·1%. The result displayed in figure 7c clearly indicates the capacity of the algorithm to detect the small change in the domain. However, because of the smallness of the distortion of the shape of the billiard, one finds eigenfunctions that are nicely symmetric (or antisymmetric) about the longest height of the triangle only up to a certain energy, because at higher energies the precision of the computation is not enough to resolve between states which originate from some pair of *degenerate* equilateral triangle eigenstates and which are either even or odd under reflection about the longest height. In fact, the algorithm yields eigenstates which are combinations of both types of eigenfunctions and therefore do not have definite parity. For the case at hand, namely a 400 × 400 matrix, we observed that all the eigenfunctions up to approximately the 50th eigenstate display the desired parity; at higher energies a transition regime takes place, where we find eigenfunctions with definite parity along with slightly distorted ones and with eigenfunctions with no parity at all (see figure 8). We also studied the same triangle using a larger matrix (600 × 600); in this case the transition regime starts approximately after the 80th eigenstate, suggesting an approximately linear scaling with the dimensions of the matrix. Unfortunately, the extensive calculations

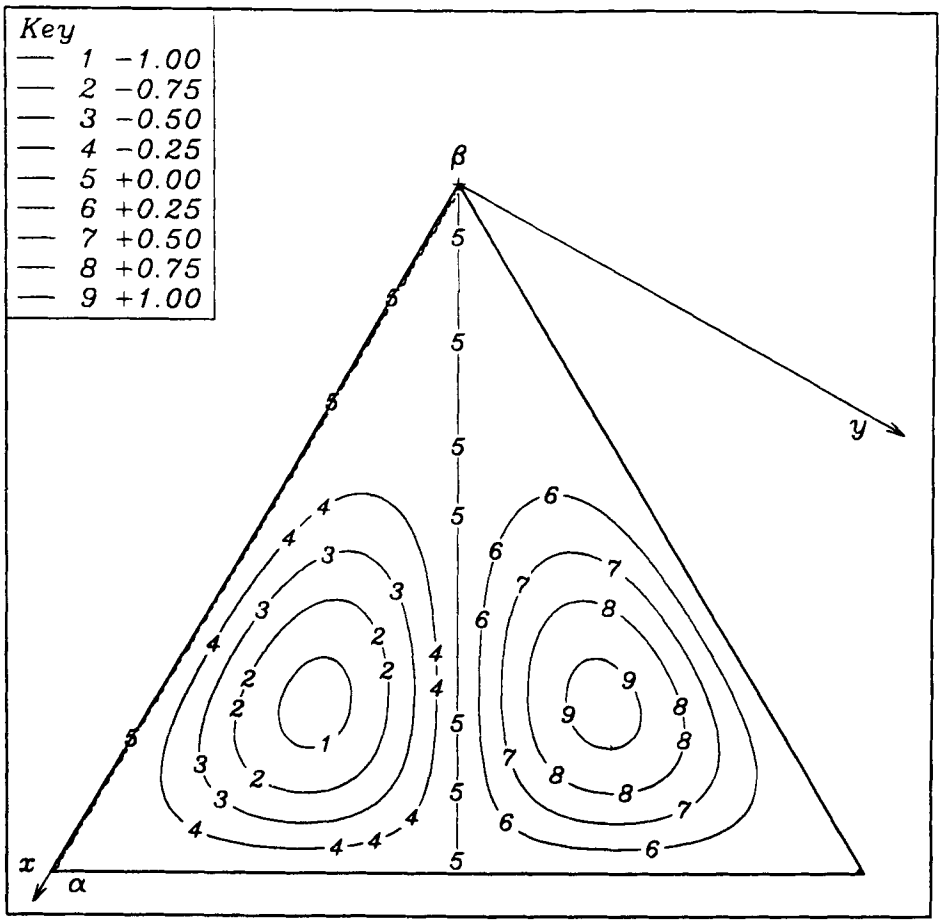

Figure 7(b).

necessary to determine the exact relationship between the dimensions of the matrix, and up to what state the eigenfunctions display well defined parity and also the size of the change in the domain, are beyond our computational reach. However, it should be noted that the problem of properly resolving quasi-degenerate states is very rare. It is well known that classically nonintegrable systems show level repulsion [1]: the energy levels of chaotic systems repel each other linearly (barring the case in which the time reversal symmetry in broken by some magnetic field), whereas some numerical evidence [15, 20] suggests that pseudointegrable systems do so according to a power law, with exponent ranging between 0·5 and 1. Therefore, degenerate or quasi-degenerate states, which are the cause of the problems encountered in the isosceles triangle, are very rare and in this case they are due to the special symmetry of the domain. Finally it can also be argued that not even the exact analytical eigenstates, because of their finite wavelength, would be able to detect very small changes in the domain of the billiard, if not in very special situations like the one at hand, which is a case of spontaneously broken symmetry.

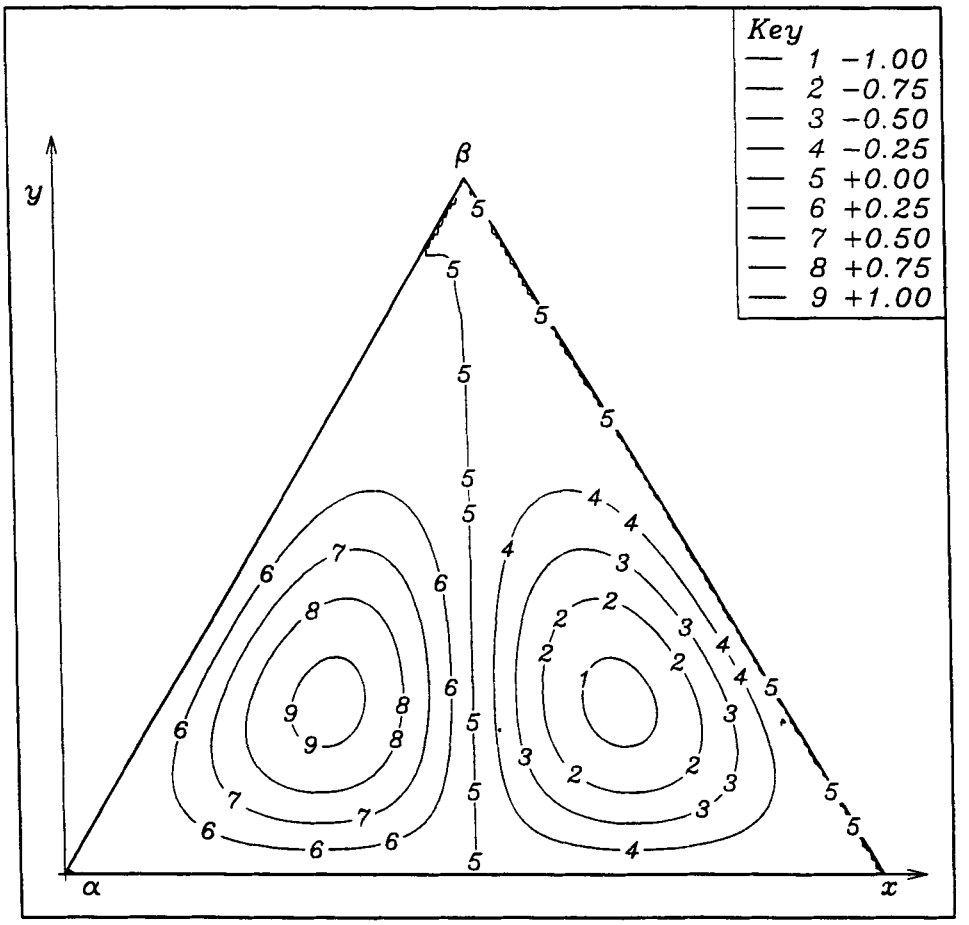

Figure 7(c).

Figure 7. Contour plot of one of the two 1st excited states (recall degeneracy) of the equilateral triangle and of an isosceles triangle; (**a**) Equilateral triangle: the calculation was performed putting the frame of reference in the lower left corner of the triangle; (**b**) Equilateral triangle: the computation was performed setting the frame of reference on the upper vertex of the triangle; (**c**) Isosceles triangle: 3rd normalized eigenstate (the removal of degeneracy energetically favors the other state of the degenerate pair); the triangle was obtained by slightly stretching the equilateral one along the height relative to the x-axis. The state was computed setting the frame of reference on the lower left corner. The result proves the capacity of the algorithm to detect small changes in the shape of the domain.

4. Conclusions

In this paper we have presented a comprehensive solution for the problem of the QBO in arbitrary triangular domains. We addressed this problem because due to its paradigmatic nature it is attracting increasing attention in the nonlinear dynamics community. Our solution requires short computing times and yields excellent results, particularly for the eigenfunctions. Moreover, it yields the eigenfunctions in a very

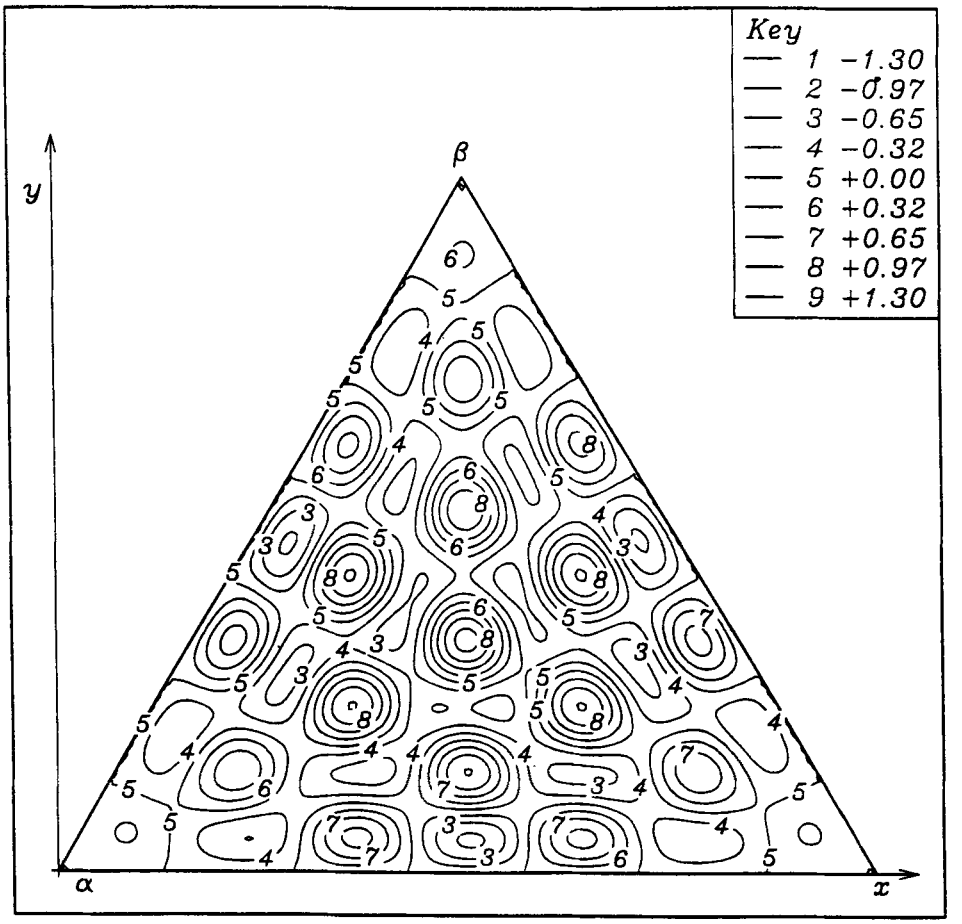

Figure 8(a).

tractable form, like (19), which allows "semi-analytical" calculations, like the one we performed in evaluating the integral (18). Such a feature offers precise, reliable and computationally economic studies of the most interesting properties of the eigenfunctions, such as investigations of the amplitude probability distribution and of the spatial correlation function and the construction of Path Correlation Functions [21] for triangular billiards. A first application of the method has led to the discovery of scars along ghosts of neutrally stable periodic orbits [12]. A more general application of the scheme and study of the statistical properties of the eigenfunctions will be presented in a forthcoming paper.

Also, the same basis set can be used with no modification to study the problem of triangular billiards in presence of some perturbing field, just by adding the matrix elements of the field to the matrix representing the laplacian; such a study would allow the study of the evolution of eigenvalues and eigenfunctions as the classical systems undergoes a transition to chaos and such studies are in progress in our group. Finally, with some small modifications the present procedure can be easily applied to the problem of quantum billiards in parallelograms: in fact, the functions obtainable simply by leaving out the antisymmetrization step are clearly a suitable Hilbert space basis for the parallelogram problem.

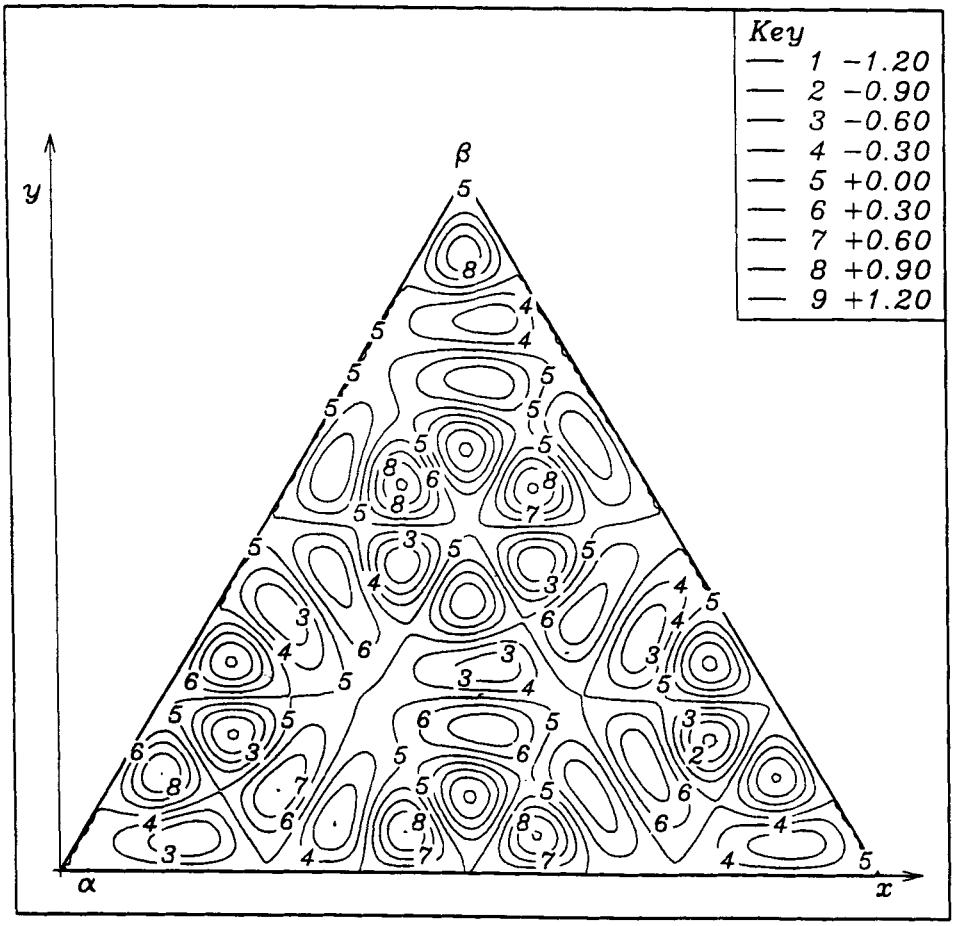

Figure 8(b).

Acknowledgements

The author wishes to thank S Bright for introducing him to Ga-tech computational facilities. He is also grateful to Prof. A Scotti who introduced him to the problem. Finally, thanks are due to Prof. T Uzer for a critical reading of the manuscript. This work was partially supported by the "Domenica Rea D'Onofrio" fellowship and by the National Science Foundation through a grant for the Institute for Theoretical Atomic and Molecular Physics at the Harvard-Smithsonian Astrophysical Observatory.

Appendix 1

Evaluation of the matrix elements

Here we give the explicit matrix elements for the QBO on an arbitrary triangular domain with base $B = a\pi$ and height $H = b\pi$: this is a larger triangle than the one

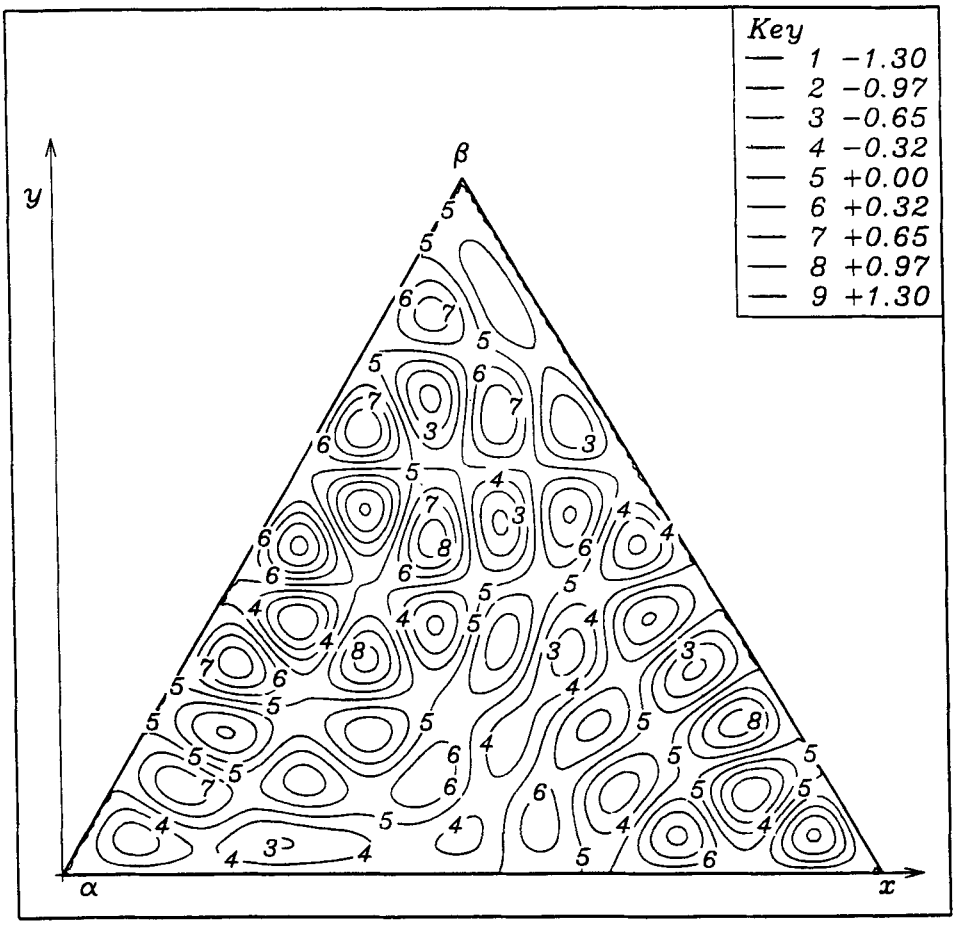

Figure 8(c).

Figure 8. Contour plots of some eigenfunctions of the isosceles triangle, computed with a 400 × 400 matrix, in the transition regime; (**a**) 57th eigenstate: the contours pattern is clearly symmetric with respect to the height of the triangle; (**b**) 59th eigenstate: the wave function shows some approximate symmetry, but is a little distorted; (**c**) 56th eigenstate: in this case every definite parity is lost and the wave function is not symmetric nor antisymmetric with respect to the height.

considered in the rest of the paper, but this simple rescaling of the sides allows us not to write a series of π's in the arguments of the basis functions keeping the notation a little less cumbersome. We will write Γ as a short for $\tan\gamma$ and we will also set $((1+\Gamma^2)/a^2) = (1/\alpha^2)$.

The matrix elements are

$$\mathscr{D}(m,n,j,k) = \frac{4}{\pi^2 ab}\iint_{\mathscr{T}} \mathrm{d}x\,\mathrm{d}y \left\{ \sin\frac{m(x-\Gamma y)}{a}\sin\frac{ny}{b} + (-1)^{m+n+1}\sin\frac{n(x-\Gamma y)}{a}\sin\frac{my}{b}\right\}$$

$$\times(-\nabla^2)\left\{\sin\frac{j(x-\Gamma y)}{a}\sin\frac{ky}{b}+(-1)^{j-k+1}\sin\frac{k(x-\Gamma y)}{a}\sin\frac{jy}{b}\right\}. \tag{A1}$$

We consider the following change of variables

$$x'=\frac{x-\Gamma y}{a} \tag{A2}$$

$$y'=\frac{y}{b}$$

which induces a transformation of the laplacian

$$\nabla^2\to\nabla^{2'}=\frac{1}{a^2}\frac{\partial^2}{\partial x'^2}+\frac{1}{b^2}\frac{\partial^2}{\partial y'^2}+\frac{\Gamma^2}{a^2}\frac{\partial^2}{\partial x'^2}-\frac{2\Gamma}{ab}\frac{\partial^2}{\partial x'\partial y'}; \tag{A3}$$

and the matrix elements reduce to

$$\begin{aligned}\mathscr{D}(m,n,j,k)=\frac{4}{\pi^2}\int_0^{\pi}dx\int_0^{\pi-x}dy\{&\sin mx\sin ny+(-1)^{m+n+1}\sin nx\sin my\}\\&\times\left\{\left[\left(\frac{j^2}{\alpha^2}+\frac{k^2}{b^2}\right)\sin jx\sin ky+(-1)^{j+k+1}\right.\right.\\&\left.\times\left(\frac{k^2}{\alpha^2}+\frac{j^2}{b^2}\right)\sin kx\sin jy\right]\\&\left.+\frac{2\Gamma}{ab}jk[\cos jx\cos ky+(-1)^{j+k+1}\cos kx\cos jy]\right\}.\end{aligned} \tag{A4}$$

We have two separate integrals, one involving sines only and the other involving cosines also

$$\mathscr{D}(m,n,j,k)=\frac{4}{\pi^2}[\mathscr{I}(m,n,j,k)+\mathscr{J}(m,n,j,k)]. \tag{A5}$$

We add the following null quantity to the sine only integral

$$(-1)^{j+k+1}\left(\frac{j^2}{\alpha^2}+\frac{k^2}{b^2}\right)\quad\{\sin kx\sin jy-\sin kx\sin jy\} \tag{A6}$$

and we obtain

$$\begin{aligned}\mathscr{I}=\left(\frac{j^2}{\alpha^2}+\frac{k^2}{b^2}\right)&\int_0^{\pi}dx\int_0^{\pi-x}dy\{\sin mx\sin ny+(-1)^{m+n+1}\sin nx\sin my\}\\&\times\{\sin jx\sin ky+(-1)^{j+k+1}\sin kx\sin jy\}+(-1)^{j+k}\left[\frac{b^2-\alpha^2}{\alpha^2b^2}(j^2-k^2)\right]\\&\times\int_0^{\pi}dx\int_0^{\pi-x}dy\{\sin mx\sin ny+(-1)^{m+n+1}\sin nx\sin my\}\{\sin kx\sin jy\}.\end{aligned} \tag{A7}$$

We can separate also $\mathscr{I}$ in two integrals

$$\mathscr{I}(m,n,j,k)=\left(\frac{j^2}{\alpha^2}+\frac{k^2}{b^2}\right)\mathscr{I}_1(m,n,j,k)+\left[\frac{b^2-\alpha^2}{\alpha^2 b^2}(j^2-k^2)\right]\mathscr{I}_2(m,n,j,k); \tag{A8}$$

the first one can be solved by using the orthonormality of the eigenfunctions of the QBO on the half square

$$\mathscr{I}_1(m,n,j,k)=\frac{\pi^2}{4}\delta_{m,j}\delta_{n,k}; \tag{A9}$$

whereas for the second one we set

$$\mathscr{I}_2(m,n,j,k)=\mathscr{I}_3(m,n,k,j)+(-1)^{m+n+1}\mathscr{I}_3(n,m,k,j) \tag{A10}$$

where

$$\begin{aligned}\mathscr{I}_3(l_1,l_2,l_3,l_4)&=\int_0^{\pi}\mathrm{d}x\int_0^{\pi-x}\mathrm{d}y\sin l_1x\sin l_2y\sin l_3x\sin l_4y\\&=\int_0^{\pi}\mathrm{d}x\int_0^{\pi-x}\mathrm{d}y\sin l_1x\sin l_3x\frac{1}{2}\{\cos[(l_2-l_4)y]\\&\qquad-\cos[(l_2+l_4)y]\},\end{aligned} \tag{A11}$$

and l_1, l_2, l_3, l_4 are integer indices which are equal to m,n,k,j in the first case and to n,m,k,j in the second; we also write

$$\mathscr{I}_3(l_1,l_2,l_3,l_4)=\mathscr{I}_4(l_1,l_2,l_3,l_4)-\mathscr{I}_4(l_1,l_2,l_3,-l_4), \tag{A12}$$

where

$$\mathscr{I}_4(l_1,l_2,l_3,l_4)=\frac{1}{2}\int_0^{\pi}\mathrm{d}x\sin l_1x\sin l_3x\int_0^{\pi-x}\mathrm{d}y\cos[(l_2-l_4)y]. \tag{A13}$$

The integral $\mathscr{I}_4$ is simple, but some care must be taken for the cases in which the arguments of the sinusoidal functions vanish. The result is

$$\mathscr{I}_4=\begin{cases}\dfrac{1}{4}\left\{\dfrac{\pi^2}{2}+\dfrac{1}{(l_1+l_3)^2}[(-1)^{l_1+l_3}-1]\right\} & \text{if } l_2-l_4=0 \text{ and } l_1-l_3=0;\\[2ex]\dfrac{1}{4}\left\{\dfrac{[(-1)^{l_1+l_3}-1]}{(l_1+l_3)^2}-\dfrac{[1-(-1)^{l_1-l_3}]}{(l_1-l_3)^2}\right\} & \text{if } l_2-l_4=0 \text{ and } l_1-l_3\neq 0;\\[2ex]\dfrac{-(-1)^{l_2-l_4}}{4(l_2-l_4)}\{\mathscr{I}_5[l_1,l_3,(l_2-l_4)]-\mathscr{I}_5[l_1,l_3,(l_4-l_2)]\} & \text{if } l_2-l_4\neq 0;\end{cases} \tag{A14}$$

and integral $\mathscr{I}_5[l_1,l_3,(l_2-l_4)]$ is defined as:

$$\mathscr{I}_5[l_1,l_3,(l_2-l_4)]=\int_0^{\pi}\mathrm{d}x\sin l_1x\cos\{[(l_3-(l_2-l_4)]x\}. \tag{A15}$$

Setting $l_5 = l_3 - (l_2 - l_4)$ we have

$$\mathcal{J}_5(l_1, l_5) = \begin{cases} \dfrac{1-(-1)^{l_1}}{l_1} & \text{if } l_5 = 0; \\ \dfrac{1-(-1)^{l_1 - l_5}}{2(l_1 - l_5)} & \text{if } l_5 \neq 0 \text{ and } l_5 + l_1 = 0; \\ \dfrac{1-(-1)^{l_1 + l_5}}{2(l_1 + l_5)} & \text{if } l_5 \neq 0 \text{ and } l_5 - l_1 = 0; \\ \dfrac{l_1[1-(-1)^{l_1 + l_5}]}{l_1^2 - l_5^2} & \text{if } l_5 \neq 0, \quad l_5 - l_1 \neq 0 \text{ and } l_5 - l_1 \neq 0; \end{cases} \tag{A16}$$

This result concludes the first part of the calculation.

We now turn to the calculation of the integral involving the cosines; we have

$$\mathcal{J}(m,n,j,k) = \frac{8\Gamma}{\pi^2 ab} jk\{\mathcal{J}_1(m,n,j,k) + (-1)^{m+n+1}\mathcal{J}_1(n,m,j,k) + (-1)^{j+k+1}\mathcal{J}_1(m,n,k,j) + (-1)^{m+n+j+k}\mathcal{J}_1(n,m,k,j)\}; \tag{A17}$$

where

$$\begin{aligned} \mathcal{J}_1(l_1,l_2,l_3,l_4) &= \int_0^{\pi} dx \int_0^{\pi - x} dy \sin l_1 x \sin l_2 y \cos l_3 x \cos l_4 y \\ &= \frac{1}{4}\int_0^{\pi} dx \{\sin[(l_1 + l_3)x] + \sin[(l_1 - l_3)x]\} \\ &\quad \times \int_0^{\pi - x} dy \{\sin[(l_2 + l_4)y] + \sin[(l_2 - l_4)y]\}, \end{aligned} \tag{A18}$$

and also

$$\begin{aligned} \mathcal{J}_1(l_1,l_2,l_3,l_4) = \{&\mathcal{J}_2(l_1,l_2,l_3,l_4) + \mathcal{J}_2(l_1,l_2,-l_3,l_4) \\ &+ \mathcal{J}_2(l_1,l_2,l_3,-l_4) + \mathcal{J}_2(l_1,l_2,-l_3,-l_4)\}, \end{aligned} \tag{A19}$$

where $\mathcal{J}_2$ is defined as:

$$\mathcal{J}_2(l_1,l_2,l_3,l_4) = \frac{1}{4}\int_0^{\pi} dx \sin[(l_1 + l_3)x] \int_0^{\pi - x} dy \sin[(l_2 + l_4)y]. \tag{A20}$$

We finally set $l_{13} = l_1 + l_3$ and $l_{24} = l_2 + l_4$ and we obtain $\mathcal{J}_2$

$$\begin{cases} 0 & \text{if } l_{13} = 0 \text{ or } l_{24} = 0; \\ \dfrac{1}{4}\left\{\dfrac{(-1)^{l_{24}}}{2l_{24}}\left[\dfrac{(-1)^{l_{13}+l_{24}}-1}{l_{13}+l_{24}}\right] + \dfrac{1-(-1)^{l_{13}}}{l_{13}l_{24}}\right\} & \text{if } l_{13} - l_{24} = 0; \\ \dfrac{1}{4}\left\{\dfrac{(-1)^{l_{24}}}{2l_{24}}\left[\dfrac{(-1)^{l_{13}-l_{24}}-1}{l_{13}-l_{24}}\right] + \dfrac{1-(-1)^{l_{13}}}{l_{13}l_{24}}\right\} & \text{if } l_{13} + l_{24} = 0; \\ \dfrac{1}{4}\left\{\dfrac{(-1)^{l_{24}}}{2l_{24}}\left[\dfrac{(-1)^{l_{13}-l_{24}}-1}{l_{13}-l_{24}} + \dfrac{(-1)^{l_{13}+l_{24}}-1}{l_{13}+l_{24}}\right] + \dfrac{1-(-1)^{l_{13}}}{l_{13}l_{24}}\right\} & \text{if } l_{13} + l_{24} \neq 0 \text{ and } l_{13} - l_{24} \neq 0; \end{cases} \tag{A21}$$

This completes the evaluation of the matrix elements.

References

[1] B Eckhardt, *Phys. Rep.* **163**, 205 (1988)
[2] I P Cornfeld, S V Fomin, Ya G Sinai, *Ergodic theory* (Springer Verlag, Heidelberg, 1980)
[3] M V Berry, *Ann. Phys. (NY)* **131**, 163 (1981)
[4] L A Bunimovich, *Commun. Math. Phys.* **65**, 295 (1979)
[5] S W McDonald and A N Kaufman, *Phys. Rev.* **A37**, 3067 (1988)
[6] R J Riddel Jr, *J. Comput. Phys.* **31**, 21 (1979)
[7] R J Riddel Jr, *J. Comput. Phys.* **31**, 42 (1979)
[8] E J Heller, in *Chaos and quantum physics*, NATO Les Houches Lecture Notes (1989)
[9] T Cheon and T D Cohen, *Phys. Rev. Lett.* **62**, 2769 (1989)
[10] D Biswas and S R Jain, *Phys. Rev.* **A42**, 3170 (1990)
[11] B Eckhardt, J Ford and F Vivaldi, *Physica* **D13**, 339 (1984)
[12] P Bellomo and T Uzer, *Phys. Rev.* **E50**, 1886 (1994)
[13] M C Gutzwiller, *Chaos in classical and quantum mechanics* (Springer Verlag, Heidelberg, 1990)
[14] H M Lauber, P Weidenhammer and D Dubbers, *Phys. Rev. Lett.* **72**, 1004 (1994)
[15] Paolo Bellomo, *Int. J. Bifurction and Chaos* (in press)
[16] R Courant and D Hilbert, *Methods of mathematical physics* (J. Wiley & Sons, New York, 1953) **vol. 1**
[17] M G Lamé, *Leçons sur la Theorie Mathematique de l' Elasticité des Corps Solides* (Bachelier, Paris, 1852)
[18] M A Pinsky, *SIAM J. Math. Anal.* **11**, 819 (1980)
[19] M V Berry and M Wilkinson, *Proc. R. Soc. London* **A356**, 15 (1984)
[20] A Shudo and Y Shimizu, *Phys. Rev.* **E47**, 54 (1993)
[21] M Shapiro and G Goelman, *Phys. Rev. Lett.* **53**, 1714 (1984)
[22] J Ford and M Ilg, *Phys. Rev.* **A45**, 6165 (1992)